

1 **Prospective Clinical Evaluation of a Deep Learning Algorithm for Guided Point-of-Care**
2 **Ultrasonography Screening of Abdominal Aortic Aneurysms**

3

4 I-Min Chiu^{1,2}, Tien-Yu Chen³, You-Cheng Zheng³, Xin-Hong Lin¹, Fu-Jen Cheng¹, David
5 Ouyang^{2*} & Chi-Yung Cheng^{1*}

6 1. Department of Emergency Medicine, Kaohsiung Chang Gung Memorial Hospital, Kaohsiung,
7 Taiwan

8 2. Department of Cardiology, Smidt Heart Institute, Cedars-Sinai Medical Center, Los Angeles,
9 CA, USA

10 3. Division of Cardiology, Department of Internal Medicine, Kaohsiung Chang Gung Memorial
11 Hospital, Kaohsiung, Taiwan

12

13 *These authors contributed equally to this manuscript.

14

15 **Short title:** Trial of Deep Learning Abdominal Aortic Aneurysm Screening

16 **corresponding author:** Chi-Yung Cheng, qzsecawsxd@cgmh.org.tw, No. 123, Dapi Rd.,

17 Niaosong Dist., Kaohsiung, 83301, Taiwan; David Ouyang, david.ouyang@cshs.org, 8700

18 Beverly Blvd, Los Angeles, CA 90048, USA

19 **Word Count:** 4188

20

21

22 **Clinical Perspective**

23

24 What is New:

- 25 • Our study presents a deep learning (DL) guidance system that enables novice users to
26 perform Abdominal Aortic Aneurysm (AAA) screening with POCUS, yielding image
27 quality comparable to experienced physicians.
- 28 • The DL algorithm accurately identifies AAA from scans conducted by novice users,
29 maintains consistent performance across patients with varying BMIs, and demonstrates
30 increased scan efficiency with repeated use.

31

32 Clinical Implications:

- 33 • DL-guided POCUS can potentially expand AAA screening capabilities to non-specialist
34 settings and increase throughput for screening at risk individuals.
- 35 • The implementation of our DL model for AAA screening could enhance early detection,
36 particularly in underserved areas, but also optimize clinical workflows by decreasing
37 diagnostic wait times and increasing ultrasound utilization efficiency.

38 **Abstract**

39 **Background:** Abdominal Aortic Aneurysm (AAA) is a critical condition that can lead to fatal
40 consequences if not detected and treated early. Despite the high prevalence in smokers and
41 guideline recommendation for screening, AAA often remains undetected due to availability of
42 diagnostic ultrasound examinations. This prospective clinical trial aimed to investigate the use of
43 a Deep Learning (DL) algorithm to guide AAA screening.

44 **Methods:** This prospective, comparative diagnostic study was conducted at the Kaohsiung
45 Chang Gung Memorial Hospital. We developed and deployed an object detection-based DL
46 algorithm providing real-time guidance for novice users performing AAA screening using point
47 of care ultrasound. 10 registered nurses with no prior ultrasonography experience were recruited
48 and performed at least 15 scans on patients over 65 years old to acquire abdominal aorta videos.
49 These scans were compared with those of physicians using the same ultrasound hardware but
50 without DL guidance.

51 **Results:** A total of 184 patients (median [IQR] age of 72 [67-79], and 105 (57.1%) male)
52 completed this study. The DL-guided novices achieved adequate scan quality in 87.5% (95% CI:
53 82.7 - 92.3%) of patients, comparable to the 91.3% (95% CI: 87.2-95.4%) rate of physician scans
54 ($p=0.310$). This performance did not vary by BMI. The DL model predicted AAA with an AUC
55 of 0.975, showing 100% sensitivity and 94.3% specificity. The DL model predicted the maximal
56 width of abdominal aorta with mean absolute error of 2.8mm compared to physician
57 measurements. 3 AAA with maximal width of aorta > 3 cm were found in this study cohort.

58 **Conclusion:** DL-guided POCUS is an effective tool for AAA screening, providing comparable
59 performance to experienced physicians. The use of this DL system could democratize AAA
60 screening and improve access, thereby aiding in early disease detection and treatment.

61 **Introduction**

62 An abdominal aortic aneurysm (AAA) is the gradual dilation of the abdominal aorta, and if left
63 untreated, it may rupture, posing a high risk of fatal consequences¹. This life-threatening
64 condition contributes to a crude mortality rate of approximately 150,000–200,000 deaths per year
65 worldwide². More than two-thirds of patients with a ruptured abdominal aortic aneurysm present
66 without a prior diagnosis of AAA³. Early detection and treatment can considerably decrease
67 AAA-related mortality, especially in the elderly⁴. Previous guidelines recommend
68 ultrasonography for general AAA screening in at-risk populations, specifically men over 65, with
69 smoking history^{5,6}.

70 Ultrasonography, the most common imaging screening modality for AAA, has proven to be
71 effective and less costly compared to standard computed tomography (CT) scans.⁷ Nonetheless,
72 ultrasound is generally performed by highly trained sonographers and interpretation carried out
73 by board-certified physicians. This challenge is further compounded by the restricted
74 accessibility of sophisticated ultrasound equipment. Both of these factors contribute to
75 ultrasound examinations having the longest waiting times compared to other imaging modalities
76 and reduce the cost-effectiveness for general screening for AAA^{8–10}.

77 In the past decade, Point-of-Care Ultrasound (POCUS) has seen extensive use across various
78 hospital settings, including outpatient clinics, emergency departments, wards, and operating
79 rooms^{11,12}. It has played a crucial role in medically underserved areas, from rural regions in
80 developed countries to low-income nations, and is even used in manned space flights¹³. Portable
81 ultrasound machines have facilitated the acquisition of high-quality images suitable for
82 diagnostic purposes¹⁴. However, the limited familiarity among hospital staff with ultrasound its
83 current utilization¹⁵. Therefore, integrating AI guidance into ultrasound could benefit novice

84 operators. This has the potential to enhance diagnostic capabilities, especially in remote areas
85 where experienced sonographers may not be readily available.

86 AI revolutionizes healthcare by rapidly interpreting images, detecting abnormalities, segmenting
87 organs and lesions, and facilitating early disease identification. Prior study suggests that AI
88 empowers individuals with no previous experience in ultrasonography to perform diagnostic
89 transthoracic echocardiographic studies, encompassing the evaluation of left and right ventricular
90 function, as well as the identification of pericardial effusion²¹. In addition, AI can guide novices
91 to capture satisfactory diagnostic images of the Morison pouch during Focused Assessment With
92 Sonography in Trauma (FAST) exam²². The objective of this study is to develop and validate a
93 Deep Learning (DL) model that guides abdominal aorta scanning and to investigate its potential
94 in assisting novices to obtain qualified scans. This approach could aid in the screening of
95 potential AAA patients by advancing the detection of symptomatic aneurysms, screening
96 asymptomatic AAAs in at-risk groups, and monitoring aneurysm growth until treatment is
97 necessary.

98

99

100

101

102

103

104

105

106

107

108 **Method**

109 *Ethical Approval*

110 The study was approved by the institutional review board at the Kaohsiung Chang Gung
111 Memorial Hospital (IRB number: 202102311B0). Written consent was obtained from each
112 participant.

113 *Development and Function of AI-Guided Image Acquisition Software*

114 The DL-guided image acquisition algorithm is detailed in the Supplemental Methods. It offers
115 real-time, continuous guidance during scanning to assist users in obtaining videos for AAA
116 screening. The software, which emulates physician expertise, utilizes a You Only Look Once
117 (YOLO) architecture, known for its real-time object detection capabilities. It is specifically
118 tailored to analyze ultrasonographic images, focusing on identifying anatomical structures
119 including the abdominal aorta, spine, and inferior vena cava (Supplemental Figure S1).

120 The algorithm operates solely based on ultrasonographic images, eliminating the need for
121 external trackers, fiducial markers, or additional sensory inputs. This streamlines the diagnostic
122 workflow and enhances screening efficiency. In this research, we installed the software on a
123 commercially available POCUS system (Telemed MicrUs EXT-1H). After integration, the
124 software monitors and processes the ultrasound display continuously through its application
125 programming interface (Supplemental Figure S2). It detects and provides the anatomical location
126 of the abdominal aorta on the ultrasound display, thereby guiding users to improve image
127 acquisition during scanning.

128 The DL algorithms were trained using 2,101 POCUS images focusing on AAA screening from
129 the studied hospital and externally validated in 492 images from a local hospital. These images
130 were retrospectively collected from routine scans conducted in the Emergency Departments
131 (EDs) of both hospitals. The performance of the algorithm achieved an average precision of
132 0.973 in internal validation and 0.843 in external validation. Supplemental Methods depicts the
133 DL model training data set, expert labeling for image quality, algorithm optimization, and
134 integration of DL system to POCUS hardware in the study.

135 *Study Design*

136 Patients at least 65 years old visiting the outpatient clinic of the Cardiology department at the
137 studied hospital were recruited between June and August 2023. Individuals were excluded if they
138 were unable to lie flat or were unable or unwilling to provide informed consent.

139 10 registered nurses without prior experience performing or interpreting ultrasonography were
140 recruited for the trial from hospital personnel. Each nurse underwent a 15-minute tutorial to
141 become familiarized with the POCUS machine and DL guidance. After that, they were asked to
142 perform 15-20 scans to acquire a 10-second standard abdominal aorta tracing video under DL
143 guidance. For control, a duplicate scan was obtained by a physician using the same POCUS
144 machine on the same day but without AI guidance. The physician also labeled the maximal width
145 of the aorta for the control scan. The nurse scans were conducted independently, solely with DL
146 guidance, and always preceded the control scans. Following each scan, the Telemed POCUS
147 machine stored two ultrasonography videos at 20 frames per second, which the DL system then
148 processed to predict the maximal width of the abdominal aorta. Figure 1 illustrates the study
149 design.

150 Upon completion of all study and control scans, a panel of 3 expert physicians (Y.C.C, X.H.L.,
151 and F.J.C.) independently and blinded to whether a nurse or a physician performed the study,
152 assessed whether each scan was of diagnostic quality, served as the primary endpoint. All expert
153 readers were certified board physicians in Cardiology or Emergency Medicine. The time to
154 complete the study, defined as the interval from placing the probe on the patient's abdomen to
155 completing the scan, was recorded. The maximal aortic width predicted by the DL model was
156 compared with expert measurements for the secondary endpoint.

157 *Statistical Analysis*

158 The study sought to evaluate the performance of nurses conducting AAA screening under DL
159 guidance, with continuous variables reported as medians and interquartile ranges (IQR), and
160 categorical variables as numbers and percentages. The proportion of qualified studies as judged
161 by the expert panel was compared between DL guidance and physician scans for the primary
162 endpoints. The maximal abdominal aortic width measurement and time to complete the study
163 were evaluated as secondary endpoints. For both primary and secondary parameters, the
164 proportion judged clinically evaluable is reported with 95% confidence intervals (CIs).

165

166

167

168

169

170

171

172 **Result**

173 During the study period, 185 patients were included. 1 patient refused to be enrolled before the
174 scan started, while 184 patients completed both the nurse and physician examinations (Figure 1).
175 Their median (IQR) age was 72 (67-79), 57.1% were male, and the median (IQR) Body Mass
176 Index (BMI) was 25.1 (23.3-28.1). 131 (71.2%) of them had Hypertension, 64 (34.8%) had
177 Diabetes Mellitus, 83 (45.1%) had heart disease, and 41 (22.3%) had a smoking history. AAA
178 was diagnosed by physicians in 3 patients, representing 1.6% of the study cohort. Table 1 shows
179 the demographics of the included patients.

180 Regarding primary outcome, no significant difference was found in the rate of qualified videos
181 between DL-guided scans 87.5% (95% CI: 82.7 - 92.3%), and physician-performed scans 91.3%
182 (95% CI: 87.2-95.4%), with p value of 0.310. Furthermore, the qualified rate for DL guidance
183 remained consistent across patients with varying BMI levels: 87.6% (95% CI: 80.9 - 94.1%) in
184 patients with BMI > 25 and 87.4% (95% CI: 80.4 - 94.3%) in patients with BMI < 25. After 5
185 rounds of examination, the proficiency of scans slightly increased, reaching an 88.1% (95% CI:
186 82.3 - 93.9%) qualification rate, as detailed in Table 2.

187 The time to complete the study was longer with DL guidance, averaging 37 seconds (IQR 21-60),
188 compared to 20 seconds (IQR 16-33) for physician-led scans (p<0.001). For nurses using DL
189 guidance, the completion time was longer in patients with a BMI over 25, taking 42 seconds
190 (IQR 27-67), as opposed to 30 seconds (IQR 18-54) for those with a BMI under 25. Physicians'
191 scan showed similar pattern between different level of BMI. With increased use of the DL

192 system, nurses' scan times decreased; after five scans, the average time was reduced from 53
193 seconds (IQR 38-82) to 30.5 seconds (IQR 18-55) as reported in Table 2.

194 Of the 161 scans under DL guidance classified as diagnostic quality, the predicted maximal
195 aortic widths showed a mean absolute error of 2.8mm compared with physician measurements,
196 as depicted in Figure 2. Of these scans, 159 (98.8%) had a discrepancy of less than 1cm when
197 compared to physician labeling. Three patients (1.6%) were diagnosed with AAA in this study
198 based on the physician's ultrasound findings. The DL model can predict AAA with an AUC of
199 0.975 (95% CI: 0.943-1). While using 2.5cm as the cut-off threshold, the DL model has 100%
200 sensitivity in detecting AAA in these patients, along with 94.3% specificity, 33.3% positive
201 predictive value, and 100% negative predictive value (Table 3).

202

203 **Discussion**

204 In this study, we developed and validated a DL algorithm for guiding novice users performing
205 AAA screening with POCUS, which notably demonstrated parity with experienced physicians in
206 producing diagnostic-quality videos. This finding suggests DL guidance can compensate for a
207 lack of extensive sonography experience, potentially broadening AAA screening accessibility.
208 Moreover, the DL model exhibited robust performance across a range of patient body mass
209 indexes and showed a notable learning curve, with improved scan times after repeated use. The
210 precision of our DL model in predicting the presence of AAA was quantitatively reflected by an
211 AUC of 0.973 in our sample population. This high level of accuracy not only demonstrates the
212 DL model's capability to distinguish between normal and pathological findings but also suggests
213 its potential as a reliable tool for early detection. These results underscore the practicality and
214 efficiency of implementing AI in clinical ultrasound practice, that may help to reduce waiting

215 time for ultrasound examination especially in resource-limited settings where access to skilled
216 sonographers is challenging.

217 The utility of POCUS is well recognized for its convenience and the immediacy with which it
218 delivers diagnostic imaging at the patient's bedside. However, its effective use is traditionally
219 limited by the operator's expertise, with the quality of the interpretation being heavily reliant on
220 the sonographer's experience. Current protocols require at least a 3-month training program for
221 technicians to become familiar with examining the abdominal aorta using ultrasound²³. This
222 presents a significant challenge in resource-limited settings where access to highly trained
223 professionals is scarce^{24,25}, which led to ongoing debate about the cost-effectiveness and
224 relevance of AAA screening. Given its low prevalence, with historical data shows the prevalence
225 rate of AAA 1.3% to 4.9 in selected risk population, the balance between the costs and benefits
226 of widespread screening is called into question^{26,27}. This is precisely where the integration of DL
227 guidance in AAA screening could play a transformative role. By potentially reducing the time
228 and expertise required for accurate screening, DL guidance can lower operational costs and
229 improve the efficiency of screening programs. Moreover, the enhanced accuracy of DL-guided
230 screening might lead to more effective identification of AAA cases even in a landscape of lower
231 prevalence, ensuring that resources are optimally utilized.

232 Advances in cardiovascular ultrasound interpretation using AI have been significant in recent
233 years, with numerous studies demonstrating automated quantification of cardiac structures and
234 function, and AI-driven disease identification showing less variability than semi-automated or
235 manual analyses²⁸⁻³¹. The convergence of AI-guided acquisition with automated interpretation
236 could expand ultrasound's reach, improving the recognition of pathology. Our study's DL

237 algorithm addresses this by providing real-time guidance to novice users, effectively bridging the
238 gap between the ease of use of POCUS and the expertise required for accurate diagnosis. By
239 supplementing the user's limited experience with sophisticated AI, we facilitate a higher standard
240 of care that could potentially revolutionize the screening process for conditions like AAA, where
241 early detection is crucial.

242 Several potential explanations for our findings emerge upon examination of the DL algorithm's
243 performance. The ability of the algorithm to offer real-time, continuous guidance likely played a
244 professional guiding role in enabling novice operators to achieve a high rate of qualified videos.
245 This real-time feedback is particularly useful during scanning, as it assists users in adjusting the
246 ultrasound probe to optimize the visualization of the aorta. Such immediate guidance can
247 improve image quality, a benefit observed in previous studies where AI support enhanced the
248 outcomes of sonography procedures, such as in the Echocardiography²¹ or Focused Assessment
249 With Sonography in Trauma exams²². The similarity between these findings and our own
250 suggests a shared advantage of AI assistance across different ultrasound applications. The
251 learning curve evidenced by the reduction in scan times with repeated use indicates that users are
252 not only becoming more adept at operating the AI system but are also gaining a better
253 understanding of the aortic structure. This suggests a synergistic enhancement in the operator's
254 ability to acquire diagnostic images, pointing to a productive interaction between human users
255 and the AI tool over time.

256 The architecture of our DL model, which delineates the abdominal aorta with a bounding box in
257 each frame of the ultrasound video, serves two critical functions. First, it offers real-time
258 feedback during the scanning process, guiding users in adjusting their probe to achieve optimal

259 imaging. Second, it enables precise diagnostic measurements post-scan. By accurately capturing
260 the anatomy of the aorta, our algorithm processes each frame to determine the aortic width,
261 subsequently calculating the maximal width from the entire video. The minimal average error of
262 2.8mm between the expert measurements and those obtained via DL guidance, along with the
263 high AUC for detecting an AAA, attest to the DL model's effective training. For further
264 evaluation, a threshold of 2.5cm led to expert review for 9 (4.9%) of the 184 scans guided by
265 DL. Within this group, three AAA cases were accurately identified, resulting in a sensitivity of
266 1.0 and a specificity of 0.94 in our cohort (Table 3). Notably, there were two scans where the
267 discrepancy in maximal width measurements between expert interpretation and DL guidance
268 exceeded 1cm (Figure 2). Manual review of these outliers showed that the DL algorithm had
269 incorrectly identified a 6.0 cm liver cyst and a 4.8 cm fluid-filled small bowel loop. These cases
270 of misclassification demonstrate that when videos with predictive diameters suspicious for AAA
271 are scrutinized, physicians can readily discern true positives from false positives.

272 **Limitations**

273 There are a few limitations of the study. First, the study was conducted in a controlled clinical
274 setting in the outpatient clinic, which allowed access to a large patient population but may not
275 fully replicate POCUS use conditions in remote or underserved areas. Second, while the sample
276 size was sufficient for the primary endpoints, the relatively small number of patients and nurses
277 limits the assessment of generalizability; larger studies could yield more robust data.
278 Additionally, there was no control group for the nurse scanners. The comparison in the study was
279 against physician's acquisitions, but an additional control group of novices untrained with the
280 algorithm was not used. Furthermore, the study location was one tertiary academic hospital.

281 Further validation across a variety of settings would help strengthen the results of the study. The
282 DL model's performance in a real-world screening scenario may differ from our controlled
283 environment. Notwithstanding these limitations, the strengths of the study included a rigorous
284 methodology, integration of the DL to the use of a commercially available POCUS system.

285 **Conclusion**

286 In conclusion, our study indicates that a DL-guided POCUS can serve as an effective tool for
287 AAA screening, achieving diagnostic accuracy that is on par with experienced physicians. This
288 innovative approach has the potential to democratize AAA screening, enhancing accessibility
289 and cost-effectiveness. By harnessing the capabilities of AI, we can streamline the screening
290 process, reduce the need for extensive sonographic training, and potentially improve patient
291 outcomes through early detection.

292

293 **Sources of Funding:**

294 This study was funded by National Science and Technology Council (MOST 111-2622-E-182A
295 001-)

296

297

298 **Reference**

- 299 1. Sakalihasan, N., Limet, R. & Defawe, O. D. Abdominal aortic aneurysm. *Lancet* **365**,
300 1577–1589 (2005).
- 301 2. Roth, G. A. *et al.* Global, regional, and national age-sex-specific mortality for 282 causes of
302 death in 195 countries and territories, 1980–2017: a systematic analysis for the Global
303 Burden of Disease Study 2017. *Lancet* **392**, 1736–1788 (2018).

- 304 3. Aggarwal, S., Qamar, A., Sharma, V. & Sharma, A. Abdominal aortic aneurysm: A
305 comprehensive review. *Exp. Clin. Cardiol.* **16**, 11–15 (2011).
- 306 4. Bains, P., Oliffe, J. L., Mackay, M. H. & Kelly, M. T. Screening older adult men for
307 abdominal aortic aneurysm: A scoping review. *Am. J. Mens. Health* **15**, 155798832110012
308 (2021).
- 309 5. Thompson, S. G., Ashton, H. A., Gao, L., Scott, R. A. P. & on behalf of the Multicentre
310 Aneurysm Screening Study Group. Screening men for abdominal aortic aneurysm: 10 year
311 mortality and cost effectiveness results from the randomised Multicentre Aneurysm
312 Screening Study. *BMJ* **338**, b2307–b2307 (2009).
- 313 6. Ashton, H. A. *et al.* The Multicentre Aneurysm Screening Study (MASS) into the effect of
314 abdominal aortic aneurysm screening on mortality in men: a randomised controlled trial.
315 *Lancet* **360**, 1531–1539 (2002).
- 316 7. Hong, H., Yang, Y., Liu, B. & Cai, W. Imaging of Abdominal Aortic Aneurysm: the
317 present and the future. *Curr. Vasc. Pharmacol.* **8**, 808–819 (2010).
- 318 8. Hofmann, B., Brandsaeter, I. Ø. & Kjelle, E. Variations in wait times for imaging services:
319 a register-based study of self-reported wait times for specific examinations in Norway.
320 *BMC Health Serv. Res.* **23**, (2023).
- 321 9. Statistics. Statistics » diagnostics waiting times and activity.
322 [https://www.england.nhs.uk/statistics/statistical-work-areas/diagnostics-waiting-times-and-](https://www.england.nhs.uk/statistics/statistical-work-areas/diagnostics-waiting-times-and-activity/)
323 [activity/](https://www.england.nhs.uk/statistics/statistical-work-areas/diagnostics-waiting-times-and-activity/).
- 324 10. Benson, R. A., Meecham, L., Fisher, O. & Loftus, I. M. Ultrasound screening for abdominal
325 aortic aneurysm: current practice, challenges and controversies. *Br. J. Radiol.* **91**, 20170306
326 (2018).

- 327 11. Lee, L. & DeCara, J. M. Point-of-care ultrasound. *Curr. Cardiol. Rep.* **22**, (2020).
- 328 12. Taylor, R. A. & Moore, C. L. Point-of-care ultrasonography of the thoracic aorta. in
329 *Emergency Point-of-Care Ultrasound* 32–38 (John Wiley & Sons, Ltd, 2017).
- 330 13. Hashim, A. *et al.* The utility of point of care ultrasonography (POCUS). *Ann. Med. Surg.*
331 *(Lond.)* **71**, 102982 (2021).
- 332 14. Dewar, Z. E. *et al.* A comparison of handheld ultrasound versus traditional ultrasound for
333 acquisition of RUSH views in healthy volunteers. *J. Am. Coll. Emerg. Physicians Open* **1**,
334 1320–1325 (2020).
- 335 15. Pinto, A. *et al.* Sources of error in emergency ultrasonography. *Crit. Ultrasound J.* **5**, (2013).
- 336 16. Shen, Y.-T., Chen, L., Yue, W.-W. & Xu, H.-X. Artificial intelligence in ultrasound. *Eur. J.*
337 *Radiol.* **139**, 109717 (2021).
- 338 17. Huang, J. *et al.* Generative artificial intelligence for chest radiograph interpretation in the
339 emergency department. *JAMA Netw. Open* **6**, e2336100 (2023).
- 340 18. Zhang, Z. & Seeram, E. The use of artificial intelligence in computed tomography image
341 reconstruction - A literature review. *J. Med. Imaging Radiat. Sci.* **51**, 671–677 (2020).
- 342 19. Qian, J., Li, H., Wang, J. & He, L. Recent Advances in Explainable Artificial Intelligence
343 for Magnetic Resonance Imaging. *Diagnostics (Basel)*. **13**, (2023).
- 344 20. Cheng, C.-Y. *et al.* Deep learning assisted detection of abdominal free fluid in Morison’s
345 pouch during focused assessment with sonography in trauma. *Front. Med. (Lausanne)* **8**,
346 707437 (2021).
- 347 21. Narang, A. *et al.* Utility of a deep-learning algorithm to guide novices to acquire
348 echocardiograms for limited diagnostic use. *JAMA Cardiol.* **6**, 624–632 (2021).

- 349 22. Chiu, I.-M. *et al.* Use of a deep-learning algorithm to guide novices in performing focused
350 assessment with sonography in trauma. *JAMA Netw. Open* **6**, e235102 (2023).
- 351 23. Hartshorne, T. C., McCollum, C. N., Earnshaw, J. J., Morris, J. & Nasim, A. Ultrasound
352 measurement of aortic diameter in a national screening programme. *Eur. J. Vasc. Endovasc.*
353 *Surg.* **42**, 195–199 (2011).
- 354 24. Becker, D. M. *et al.* The use of portable ultrasound devices in low- and middle-income
355 countries: a systematic review of the literature. *Trop. Med. Int. Health* **21**, 294–311 (2016).
- 356 25. Shaddock, L. & Smith, T. Potential for use of portable ultrasound devices in rural and
357 remote settings in Australia and other developed countries: A systematic review. *J.*
358 *Multidiscip. Healthc.* **15**, 605–625 (2022).
- 359 26. Thompson, S. G., Ashton, H. A., Gao, L., Buxton, M. J. & Scott, R. A. Multicentre
360 Aneurysm Screening Study (MASS) Group. Final follow-up of the multicentre aneurysm
361 screening study (MASS) randomized trial of abdominal aortic aneurysm screening. *Br J*
362 *Surg* **99**, 1649–1656 (2012).
- 363 27. McCaul, K. A., Lawrence-Brown, M., Dickinson, J. A. & Norman, P. E. Long-term
364 outcomes of the western Australian trial of screening for abdominal aortic aneurysms:
365 Secondary analysis of a randomized clinical trial. *JAMA Intern. Med.* **176**, 1761–1767
366 (2016).
- 367 28. Ouyang, D. *et al.* Video-based AI for beat-to-beat assessment of cardiac function. *Nature*
368 **580**, 252–256 (2020).
- 369 29. Duffy, G. *et al.* High-throughput precision phenotyping of left ventricular hypertrophy with
370 cardiovascular deep learning. *JAMA Cardiol.* **7**, 386–395 (2022).

371 30. Wu, C. C., Cheng, C. Y., Chen, H. C., Hung, C. H. & Chen, T. Y. Development and
372 validation of an end-to-end deep learning pipeline to measure pericardial effusion in
373 echocardiography. *medRxiv* (2022).

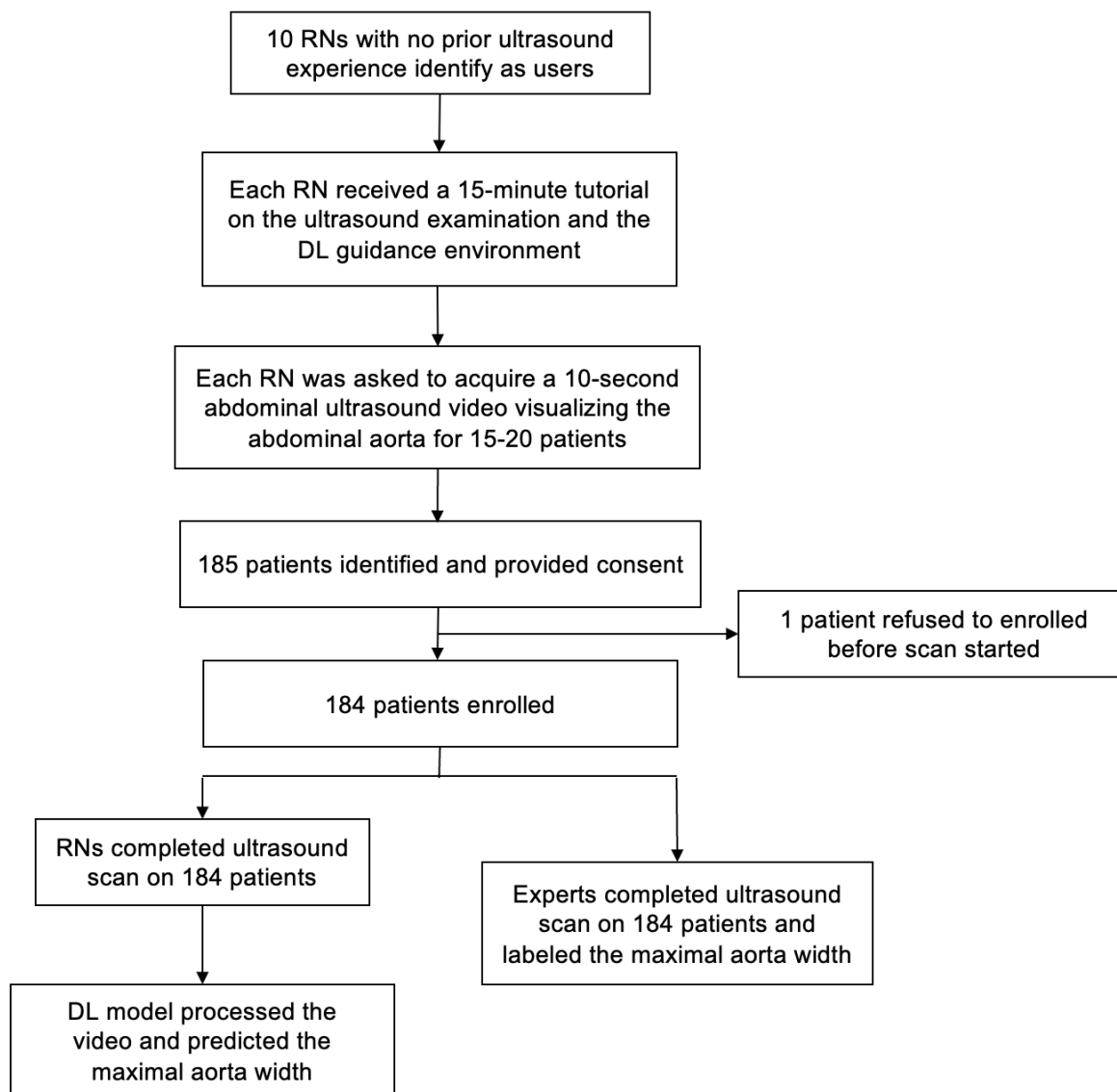
374 31. Madani, A., Ong, J. R., Tibrewal, A. & Mofrad, M. R. K. Deep echocardiography: data-
375 efficient supervised and semi-supervised deep learning towards automated diagnosis of
376 cardiac disease. *NPJ Digit. Med.* **1**, 59 (2018).

377

378

379

380 Figure 1. Study design.

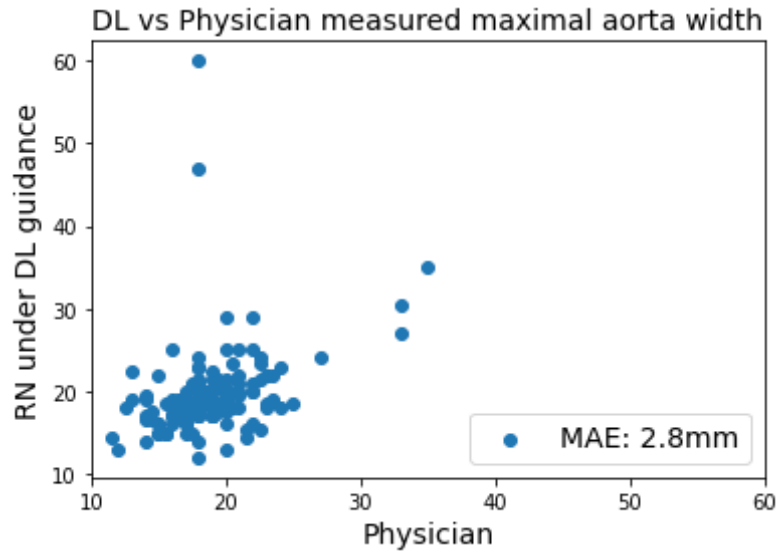


381

382

383

384 Figure 2. Scatter Plot of Maximal Aortic Width Measurements by Deep Learning Predictions and
385 Physician Labels



386
387

388 Table 1. Demographic of included patients.

	Median (IQR) / N (%)
Total patients	184
Age	72 (67-79)
Male	105 (57.1%)
BMI	25.1 (23.3-28.1)
Underlying disease	
Hypertension	131 (71.2%)
DM	64 (34.8%)
Heart disease	83 (45.1%)
PAOD	1 (0.5%)
CKD	24 (13.0%)
Abdominal operation	48(26.1%)
Smoking	41(22.3%)
Family history	
Heart disease	31 (16.8%)
Aortic disease*	1 (0.5%)
AAA	3 (1.6%)

389 DM=Diabetes Mellitus; PAOD=Peripheral Artery Occlusive Disease; CKD=Chronic Kidney Disease;

390 *AAA or Aortic dissection

391

392

393

394 Table 2. Comparison of Nurse-Acquired and Physician-Acquired Studies for Primary and Secondary
 395 Clinical Parameters

	Physician	DL guidance	p-value
Qualified Video	No. (%) [95% CI]		
Total	168 (91.3) [87.2 - 95.4]	161 (87.5) [82.7 - 92.3]	0.310
BMI>25 (N=97)	91 (93.8) [87.6 - 99.8]	85 (87.6) [80.9 - 94.1]	0.137
BMI<25 (N=87)	77 (88.5) [81.5 - 95.4]	76 (87.4) [80.4 - 94.3]	0.816
Before 5 scans (N=50)	45 (90.0%) [81.7-98.3]	43 (86.0%) [76.4-95.6]	0.613
After 5 scans (N=134)	123 (91.8) [86.5 – 97.1]	118 (88.1) [82.3 - 93.9]	0.659
Time to Complete Study	Median (IQR), Seconds		
total	20 (16-33)	37 (21-60)	<0.001
BMI>25 (N=97)	21 (16-35)	42 (27-67)	
BMI<25 (N=87)	18 (15-28)	30 (18-54)	
Before 5 scans (N=50)	20 (16-35)	53 (38-82)	
After 5 scans (N=134)	20 (15-30)	30.5 (18-55)	

397 Table 3. Diagnostic performance for predicting AAA by DL algorithm.

	DL-guidance
AUC	0.975 (0.943-1)
Sensitivity	100%
Specificity	94.4%
Positive Predictive Value	33.3%
Negative Predictive Value	100%

398

399

400

401 **Supplemental Material**

402 **Supplemental Methods.** Development of the DL-Guidance Algorithm

403 **Table S1.** DL model performance in internal and external validation.

404 **Figure S1.** An example of label over abdominal aorta, spine, and inferior vena cava.

405 **Figure S2.** User interface of the DL guidance for image acquisition on POCUS.

406 **Videos S1.** Demo of real-time bounding box guidance displayed on POCUS.

407

408

409 **Supplemental Methods**

410 **Data Curation:** For developing the DL model, we collected ultrasound images from the
411 ultrasound machines, include Sonosite Edge II and Hitachi Noblus, in the ED of Kaohsiung
412 Chang Gung Hospital from Jan 2019 to Dec 2021. Ultrasound images focusing on abdominal
413 area were collected. Images that were not related to abdominal aorta examination were excluded
414 and eventually a dataset comprising 2,101 labeled ultrasound images was used. We also
415 collected 492 ultrasound images from a regional hospital for external validation.

416 Each ultrasound image was cropped into 600*400 in size and get rid of the information that may
417 reveal personal identification. Two medical experts on point of care ultrasound then manually
418 labeled the selected anatomical structures - the aorta, inferior vena cava (IVC), and spine (Figure
419 S1) with polygon mask. We adopted 6 commonly used labeling software, Labelme, for this study
420 and save the labeling file under COCO dataset format. This large, annotated dataset served as the
421 foundation for training the AI models, enabling them to recognize and correctly identify these
422 structures in ultrasound images.

423 **DL Model Development and Validation:** Two DL models were developed. The first was an
424 object-detection-based AI model aim to provide real-time feedback and the second was trained to
425 automatically identify and outline the aorta, inferior vena cava, and spine within each frame of
426 the ultrasound video. These models were trained and initially validated using the annotated
427 dataset, reserving a portion for later testing. The first architecture employed in our study is
428 YOLOv5 instance segmentation. The input is an ultrasound image with a resolution of 600 x 600,
429 and the inference output includes bounding boxes and pixel area identification for each category
430 (abdominal aorta, spine, and inferior vena cava). As the original ultrasound images vary in size,
431 we opted for the 'letterbox' preprocessing method to standardize them to the model's required

432 dimensions. Letterboxing scales the image while maintaining the original aspect ratio; any
433 remaining space after scaling is filled with the background, mimicking the effect of placing a
434 picture into an envelope, hence the term 'letterbox'. YOLOv5, in terms of its architecture,
435 originates from YOLOv4's CSPDarknet53, and incorporates several improvements to enhance
436 speed and inference outcomes. For instance, it replaces the Spatial Pyramid Pooling (SPP) with
437 SPPF to boost computational speed and utilizes techniques such as Copy-Paste for data
438 augmentation. The result of validation was shown in Table S1.

439 **Integrated DL model with POCUS:** The POCUS equipment used in this study is the ArtUs-
440 EXT-1H from Telemed, a FDA-certified platform for capturing raw ultrasound signals. It can be
441 used in conjunction with a portable tablet computer. The tablet runs on a Windows 11
442 environment and uses an Intel CPU (detailed specifications are listed below). To accelerate the
443 inference speed of the deployed model, the trained YOLOv5 model was converted from the
444 PyTorch (.pt) format to the OpenVINO IR (FP16) format and utilized via OpenVINO Runtime.
445 We used Python's built-in ctypes library to load the dll (dynamic link library) provided by
446 Telemed, allowing real-time ultrasound images to be captured within the Python program. The
447 program also allows for model inference and uses OpenCV to visually represent the identified
448 Aorta (Figure S2). Additionally, to accommodate for the need to adjust parameters such as TGC
449 (time gain compensation) during scanning, a control panel interface is displayed using Tkinter
450 for the operator to adjust as necessary.

451

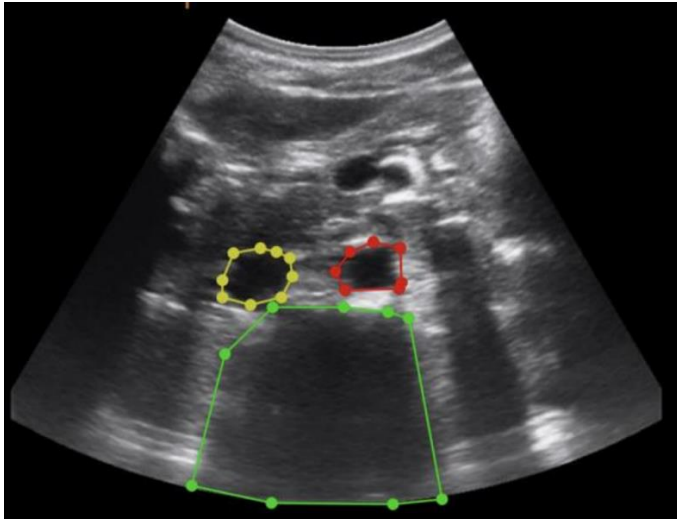
452 Table S1. DL model performance in internal and external validation.

	Box Precision	Box Recall	Box mAP@0.5
Internal Validation	0.921	0.987	0.973
External Validation	0.627	0.943	0.843

453

454

455 Figure S1. An example of label over abdominal aorta, spine, and inferior vena cava.

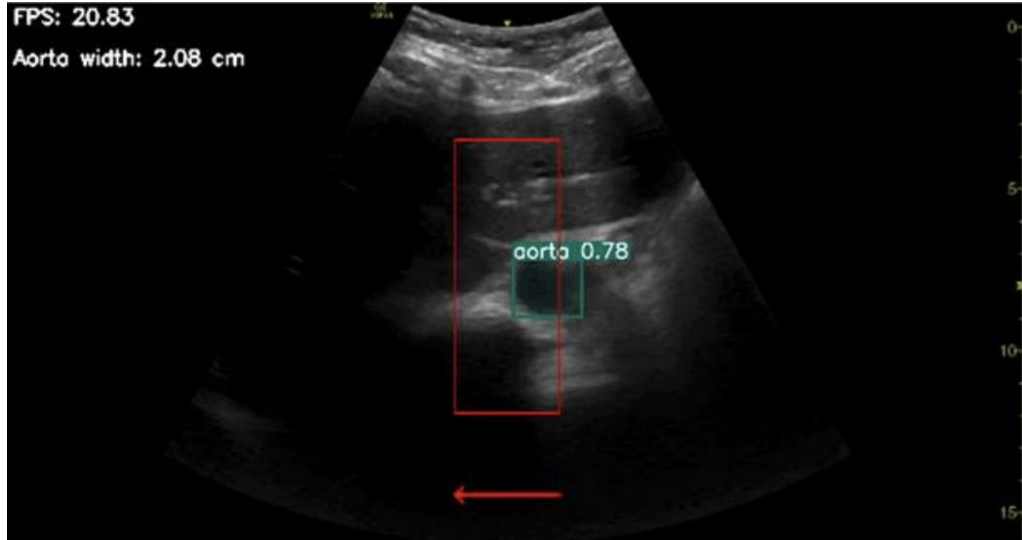


456

457

458

459 Figure S2. user interface of the DL guidance for image acquisition on POCUS



460